

# Frequency conversion in compositionally graded PPLN crystals

V.V. Galutskiy, E.V. Stroganova, S.A. Shmargilov, N.A. Yakovenko

**Abstract.** This paper considers the effect of the longitudinal lithium concentration distribution in PPLN converters on their efficiency in high-power cw laser second harmonic generation.

**Keywords:** PPLN, compositionally graded crystal, lithium niobate.

Periodically poled lithium niobate (PPLN) structures are successfully used for laser second harmonic generation, instead of bulk lithium niobate nonlinear optical converters [1]. This approach is particularly effective in converting the output of cw fibre and semiconductor lasers and in designing parametric oscillators [2]. However, when PPLN is used as a nonlinear optical element in second harmonic generation with high-power cw lasers for producing a bright, contrast picture in applications such as projection television and other multimedia devices, photorefractive damage is a significant limiting factor [3, 4]. The photorefractive damage threshold of PPLN can be raised by doping the crystalline host with Mg, In, or Sr, or by switching from PPLN to periodically poled lithium tantalate (PPLT) [4].

Another, no less important factor limiting the use of PPLN in nonlinear optical conversion of the output of high-power cw lasers is the intrinsic absorption in this crystalline material. It is known [5] that increasing the pump power leads to a temperature field redistribution in PPLN, with the result that its working temperature differs from that corresponding to the maximum conversion efficiency. Moreover, at some critical pump power, the pump conversion efficiency ensured by PPLN, e.g. second harmonic generation efficiency, decreases in an oscillating manner [5, 6].

In this paper, we examine the possibility of improving the efficiency of PPLN converters through the use of compositionally graded nonlinear optical media. Previously [7, 8], a crystal growth process was proposed in which the composition of a crystal, or the doping level, was varied in a controlled way during pulling [7, 8]. Variations in composition during pulling should lead to a phase velocity mismatch between interacting waves in PPLN, compensation of the induced wave vector mismatch (at a constant domain grating period) and, as a consequence, a reduction in the thermal effect of the intrinsic absorption in the crystalline material.

To analyse the effect of an axial composition gradient in PPLN on the efficiency of 1.06- $\mu\text{m}$  pump conversion to the second harmonic, we used a configuration in which a PPLN bar  $1 \times 1 \times 8$  mm in dimensions was situated in a metallic box. The temperature in the box was maintained constant at 30 °C by an external temperature controller (Fig. 1).

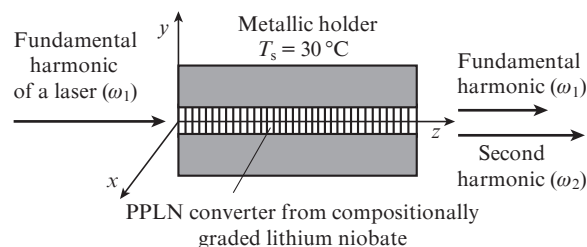


Figure 1. PPLN converter schematic.

To model the temperature effect on light propagation along the PPLN axis, we used standard second harmonic generation equations [5]:

$$\frac{dA_1}{dz} = \frac{8\pi i \omega_1^2}{k_1 c^2} d(z) A_2 A_1^* \exp(-i\Delta k z) - 0.5\alpha_1 A_1, \quad (1)$$

$$\frac{dA_2}{dz} = \frac{4\pi i \omega_2^2}{k_2 c^2} d(z) A_1^2 \exp(i\Delta k z) - 0.5(\alpha_2 + \beta A_2 A_2^*) A_2,$$

where  $k_{1,2} = n_{1,2}\omega_{1,2}/c$ ,  $n_{1,2}$ ,  $\omega_{1,2}$  and  $\alpha_{1,2}$  are the wavenumbers, refractive indices, frequencies and intrinsic absorption coefficients of the crystalline material for the fundamental and second harmonics, respectively;  $\Delta k = 2k_1 - k_2$  is the magnitude of the wave vector mismatch between the pump and second harmonic waves;  $\beta$  is the two-photon absorption coefficient for the second harmonic;  $d(z) = d_{\text{eff}} \text{sign} \cos(2\pi/\Lambda)$ ;  $d_{\text{eff}} = 16$  pm  $\text{V}^{-1}$  is the effective nonlinearity coefficient;  $\Lambda$  is the regular domain structure period;

$$A_1 = \left[ \frac{2\pi I_0 f_1(x, y) f_2(t)}{n_1 c} \right]^{1/2} \quad \text{and} \quad A_2 = 0$$

are the input amplitudes of the pump and second harmonic waves, respectively;  $I_0$  is the initial intensity of the first harmonic;  $f_1(x, y) = \exp[-(x^2 + y^2)/r_0^2]$  is the input laser pump intensity distribution;  $r_0$  is the beam radius;  $f_2(t) = 1$  and  $f_2(t) = \exp[-(t - t_0)^2/\tau^2]$  are the time functions for continuous and

V.V. Galutskiy, E.V. Stroganova, S.A. Shmargilov, N.A. Yakovenko  
Kuban State University, Stavropol'skaya ul. 149, 350040 Krasnodar,  
Russia; e-mail: Galutskiy17v@mail.ru

Received 23 July 2013; revision received 16 October 2013  
Kvantovaya Elektronika 44 (1) 30–33 (2014)  
Translated by O.M. Tsarev

pulsed laser pumping;  $\tau$  is the pump pulse duration; and  $t_0$  is the instant at which the pump pulse begins.

Local pump and second harmonic intensities are given by

$$I_{1,2}(x, y, z, t) = \frac{n_{1,2} c}{2\pi} |A_{1,2}(x, y, z, t)|^2. \quad (2)$$

The absorption of light in the PPLN by the crystalline material with absorption coefficients  $\alpha_1 = 0.002 \text{ cm}^{-1}$  and  $\alpha_2 = 0.025 \text{ cm}^{-1}$  and a two-photon absorption coefficient  $\beta = 5 \times 10^{-11} \text{ m W}^{-1}$  causes heating of the PPLN. The temperature field in the PPLN can be taken into account by numerically solving, using the finite element method, the heat equation

$$\rho C \frac{\partial T}{\partial t} = K \nabla^2 T + q(x, y, z, t), \quad (3)$$

where  $\rho = 4600 \text{ kg m}^{-3}$ ,  $C = 650 \text{ J kg}^{-1} \text{ K}^{-1}$  and  $K = 4.6 \text{ W m}^{-1} \text{ K}^{-1}$  are the density, specific heat and thermal conductivity of lithium niobate [5] and  $q(x, y, z, t)$  represents heat sources. At the end faces of the PPLN, heat exchange is with air, and the boundary conditions have the form  $-K \nabla T = h(T - T_0)$ , where  $h = 10 \text{ W m}^{-2} \text{ K}^{-1}$  is the heat exchange coefficient of lithium niobate in air at  $T_0 \approx 20^\circ \text{C}$ . In solving the heat equation, we used a  $30 \times 30 \times 20$  computational mesh and 400 points for time discretisation. The temperature values obtained were linearly interpolated for the system of Eqns (1), in which we used a  $30 \times 30 \times 500$  mesh.

The heat source distribution in the PPLN was represented by

$$\begin{aligned} q(x, y, z, t) &= -\frac{d}{dz} [I_1(x, y, z, t) + I_2(x, y, z, t)] \\ &= \alpha_1 I_1 + \alpha_2 I_2 + \beta I_2^2. \end{aligned} \quad (4)$$

Since the phase velocity mismatch curve for PPLN is determined not only by its temperature but also by its composition, because its refractive index depends on wavelength, crystal temperature and lithium concentration [9], in our studies we analysed various lithium (or niobium) concentration profiles in the lithium niobate crystal before poling.

To this end, various lithium concentration distributions along the PPLN axis (Fig. 2) were introduced into Eqns (1). In all the distributions, the average lithium concentration in

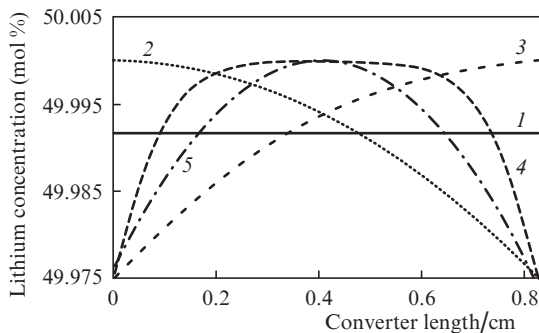


**Figure 2.** Axial lithium concentration profiles examined: (1) constant lithium concentration in the PPLN crystal, (2) parabolically decreasing concentration, (3) rising as a hyperbolic tangent, (4) in the form of a hyperbolic tangent, (5) parabolic.

the PPLN was 49.9916 mol %. It is for this concentration that we calculated the wave vector mismatch between interacting waves, and the mismatch was compensated for by the regular domain structure period  $\Lambda = 2\pi/(2k_1 - k_2)$  at a temperature of  $30^\circ \text{C}$ .

Figure 3 shows the efficiencies of the converters made from crystals with the above lithium profiles. It is seen that a parabolic decrease in lithium concentration along the PPLN axis has an adverse effect on conversion efficiency: at pump powers above 35 W, the efficiency is almost zero. On the whole, the second harmonic power at the output of the PPLN is in this instance lower than that at a constant lithium concentration over the entire range of cw laser pump powers examined. At the same time, conversion efficiency in the PPLN made from a crystal with the lithium concentration rising as a hyperbolic tangent is higher than that in the PPLN made from a crystal with a constant lithium concentration. The constant lithium concentration is equal to the average lithium concentration in a compositionally graded converter, and the periods of the PPLN structures used correspond to zero mismatch just at this lithium concentration.

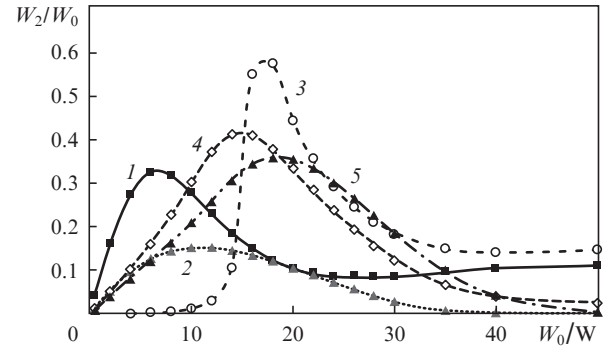


**Figure 3.** PPLN converter efficiencies corresponding to the lithium concentration profiles in Fig. 2.  $W_0$  and  $W_2$  are the pump and second harmonic powers.

It is known [5] that, when there is no temperature effect, conversion efficiency is considerably higher and is only limited by partial withdrawal of the pump and second harmonic radiation from the conversion process via the intrinsic absorption in the lithium niobate.

If temperature effects are taken into account when the pump power exceeds some threshold (10 W in our case), conversion efficiency experiences damped oscillations, dropping to 10% at a pump power of 50 W.

This sharp decrease in conversion efficiency is caused by the temperature effect. Local heating of the PPLN in the beam propagation direction changes the phase matching condition for interacting fundamental (pump) and second harmonic waves. The change in phase matching condition is equivalent to a change in refractive indices along the propagation direction of the interacting beams, i.e. to so-called thermal lensing. Figure 4 illustrates thermal lensing at a pump power of 18 W in PPLN containing 49.9916 mol % Li.

It is seen in Fig. 4a that the index difference profile for the pump wave and its second harmonic has a ‘hump’ 0.5 cm from the end face of the PPLN bar, which means that the central part of the converter is optically denser. Taking into account the longitudinal variation in refractive index along the PPLN in our model leads to refraction of the pump and

second harmonic beams, deviation from the phase matching condition and, as a consequence, a reduction in conversion efficiency. As seen in Figs 3 and 4, a thermally activated hump in the index difference profile emerges not at once but starting at some pump power. Before this critical change in index difference, the power at the output of the PPLN increases, the hottest part of the converter is its back end (primarily because of the two-photon absorption), and the temperature varies monotonically along the converter axis (as does the refractive index difference).

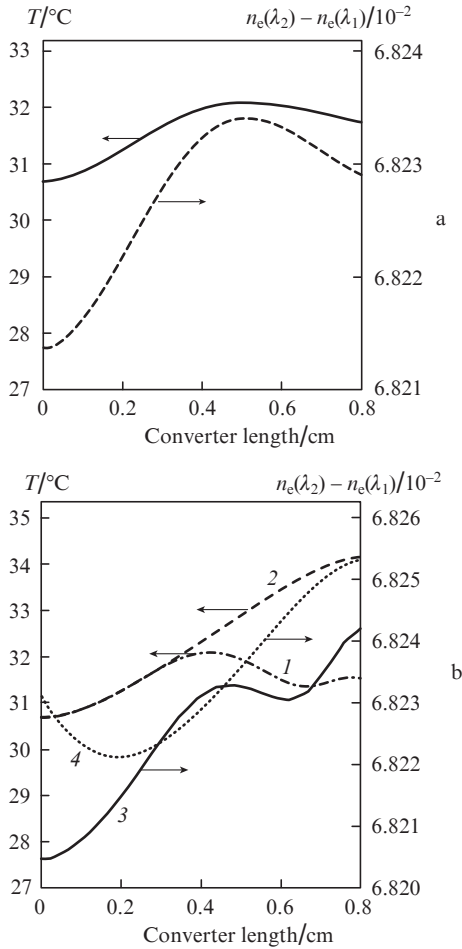


**Figure 4.** Temperature and index difference profiles along the PPLN axis at  $W_0 = 18$  W for extraordinary pump and second harmonic waves: (a) constant lithium concentration in the PPLN, (b) (1, 3) parabolically decreasing concentration, (2, 4) concentration rising as a hyperbolic tangent.

At the same time, the occasionally higher efficiency of the compositionally graded PPLN converter can be accounted for by the compensation of such thermally activated optical distortions in the compositionally graded crystal in the range of pump powers used. Figure 4b shows temperature profiles along the PPLN axis and the corresponding index difference profiles for pump and second harmonic waves at various lithium concentration profiles.

It is seen in Fig. 4b that, when the lithium concentration decreases along the PPLN axis, the index difference profile has not one but two thermally induced humps, in contrast to that in the case of constant lithium concentration in PPLN. When the lithium concentration rises as a hyperbolic tangent,

there are also thermo-optic distortions, but with no maxima. The lithium concentration gradient along the PPLN axis then compensates for the variation in the index difference between the interacting waves so that the temperature increases monotonically along the length of the PPLN, indicating an increase in second harmonic power. In the model we use, the increase in temperature is mainly due to two-photon absorption at the second harmonic frequency. The overall reduction in the efficiency of the PPLN converter when the lithium concentration in it increases as a hyperbolic tangent is attributable to the fact that the refractive indices for extraordinary pump and second harmonic waves increase with temperature at different rates, which is particularly evident when the index difference between the interacting waves is considered.

Figure 5 shows temperature profiles along the PPLN axis at different instants of time. It is seen that the temperature relaxation time in PPLN, estimated at 0.3–1 s, is consistent with the present results: the temperature distribution along the converter axis stabilises in 200–300 ms.

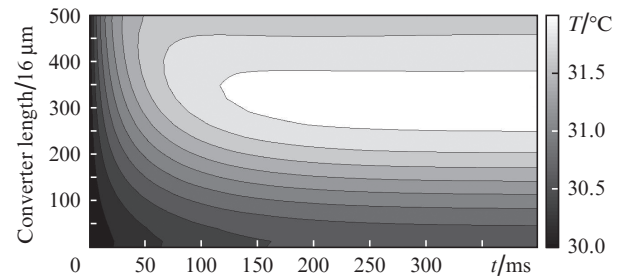


**Figure 5.** Temperature profiles along PPLN with constant lithium concentration at different instants of time (temperature step, 0.2°C). The pump pulse begins at  $t_0 = 0$ .

In the geometry under consideration and in the range of pump powers examined, the temperature distribution along the PPLN axis stabilises in 0.2–0.3 s both at a constant lithium concentration and in compositionally graded PPLN. Figure 6 illustrates the time variation of the output Gaussian second harmonic beam power profile normalised to the pump power. It is seen that the conversion efficiency is first at its maximum level and then decreases to a lower level as the PPLN heats up and stabilises.

Thus, the conversion of the output of high-power cw lasers by PPLN converters in the form of compositionally graded lithium niobate crystals may be several times as efficient as that by PPLN converters from conventional, opti-

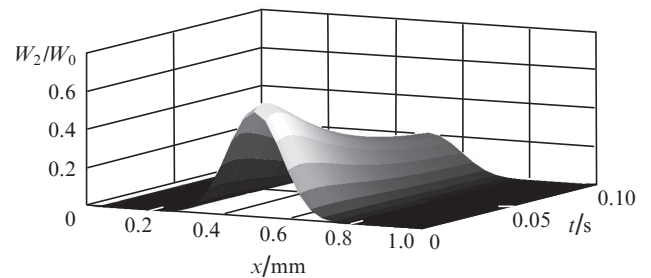


**Figure 6.** Second harmonic power  $W_2$  normalised to the pump power ( $W_0 = 18$  W) at the output of compositionally graded PPLN with a lithium concentration profile in the form of a hyperbolic tangent at different instants of time.

cally homogeneous lithium niobate crystals. In the former case, however, higher conversion efficiencies occur in a narrower range of pump powers, which is caused by a possible nonlinear variation in the phase difference between the interacting waves.

**Acknowledgements.** This work was supported through the Kuban State University Strategic Development Programme.

## References

1. Zhao H., Sukhoy K., Lima I.T. Jr., Major A. *Laser Phys. Lett.*, **9**, 355 (2012).
2. Kolker D.B., Dmitriev A.K., Gorelik P., Vong F., Zondy J.J. *Kvantovaya Elektron.*, **39**, 431 (2009) [*Quantum Electron.*, **39**, 431 (2009)].
3. Dmitriev V.G., Tarasov L.V. *Prikladnaya nelineinaya optika* (Applied Nonlinear Optics) (Moscow: Fizmatlit, 2004).
4. Sidorov N.V., Volk T.R., Mavrin B.N., Kalinnikov V.T. *Niobat litiya. Defekty. Fotorefraktsiya. Kolebatel'nyi spektr. Polyaritony* (Lithium Niobate: Defects, Photorefraction, Vibrational Spectrum and Polaritons), (Moscow: Nauka, 2003).
5. Louchev O.A., Yu Nan Ei, Kurimura Sunao, Kitamura Kenji. *Appl. Phys. Lett.*, **87**, 131101 (2005).
6. Pavel N., Shoji I., Taira T., Mizuuchi K., Morikawa A., Sugita T., Yamamoto K. *Opt. Lett.*, **29**, 830 (2004).
7. Galutskiy V.V., Vatlina M.I., Stroganova E.V. *J. Cryst. Growth*, **311**, 1190 (2009).
8. Galutskii V.V., Stroganova E.V., Yakovenko N.A. *Opt. Spektrosk.*, **110**, 436 (2011).
9. Schlarb U., Betzler K. *Ferroelectrics*, **156**, 99 (1994).